Antitumor activity of CTFB, a novel anticancer agent, is associated with the down-regulation of nuclear factor-κB expression and proteasome activation in head and neck squamous carcinoma cell lines

Sergej Skvortsov,[1] Ira Skvortsova,[2] Taras Stasyk,[3] Natalia Schiefermeier,[3] Andreas Neher,[4] Andreas R. Gunkel,[4] Guenther K. Bonn,[5] Lukas A. Huber,[3] Peter Lukas,[2] Christopher M. Pleiman,[6] and Heinz Zwierzina[1]

Departments of [1]Internal Medicine, [2]Therapeutic Radiology and Oncology, [3]Biocenter, Division of Cell Biology; [4]Department of General Otorhinolaryngology, Innsbruck Medical University, [5]Institute of Analytical Chemistry and Radiochemistry, Leopold-Franzens University, Innsbruck, Austria; and [6]Myriad Pharmaceuticals Inc., Salt Lake City, Utah

Abstract

This study aimed to characterize the antitumor activity of 5-Chloro-N-{2-[2-(4-chloro-phenyl)-3-methyl-butoxy]-5-trifluoromethyl-phenyl}-2-hydroxy-benzamide (CTFB), a novel anticancer agent, in head and neck cancer cell lines, FaDu, SCC-25 and cisplatin-resistant CAL-27. CTFB was generated as a result of an extensive medicinal chemistry effort on a lead compound series discovered in a high-throughput screen for inducers of apoptosis. All cell lines showed significant growth delay in response to CTFB treatment at a concentration of 1 μmol/L with 17.16 ± 2.08%, 10.92 ± 1.22%, and 27.03 ± 1.86% of cells surviving at 120 h in FaDu, CAL-27, and SCC-25, respectively. To define proteins involved in the mechanism of action of CTFB, we determined differences in the proteome profile of cell lines before and after treatment with CTFB using two-dimensional difference gel electrophoresis followed by computational image analysis and mass spectrometry. Eight proteins were found to be regulated by CTFB in all cell lines. All these proteins are involved in cytoskeleton formation and function and/or in cell cycle regulation. We showed that CTFB-induced cell growth delay was accompanied by cell cycle arrest at the G_0-G_1 phase that was associated with the up-regulation of p21/WAF1 and p27/Kip1 expression and the down-regulation of cyclin D1. Furthermore, we showed that activity of CTFB depended on the down-regulation of nuclear factor-κB (NF-κB) and NF-κB p65 phosphorylated at Ser^{536}. The level of proteasome activity correlated with the response to CTFB treatment, and the down-regulation of NF-κB is accompanied by enhanced proteasome activity in all investigated head and neck cancer cell lines. In this report, we show that CTFB reveals multiple effects that lead to delayed cell growth. Our data suggest that this compound should be studied further in the treatment of head and neck cancer. [Mol Cancer Ther 2007;6(6):1898–908]

Introduction

Head and neck squamous cell carcinoma (HNSCC) is a major cause of cancer-associated mortality and makes up about 6% of all cancers worldwide (1). Progress in surgical and radiotherapeutic techniques and advances in chemo- and molecular targeted therapy during the past 10 years have improved the outcome of HNSCC patients. Recently, cetuximab, an antibody directed against the epidermal growth factor receptor (EGFR) in combination with chemotherapy (2, 3) or radiotherapy (4) has been shown to improve locoregional control and to reduce mortality in locally advanced and metastatic HNSCC patients. Disease control can be achieved in a considerable number of patients that was shown among 87 trials. However, the use of chemotherapy and chemoradiotherapy is associated with a survival advantage of only 5% and 8% at 5 years, respectively (5, 6). Primary and secondary resistance to chemotherapeutics contributes to poor clinical outcomes in head and neck cancer patients. Various mechanisms are involved in the development of chemoresistance, such as AKT up-regulation (7), increased expression of Bcl-2 (8) and nuclear factor-κB (NF-κB) (9). Moreover, chemoresistance can be induced by a cellular function of the MDR1 gene that actively purges drugs from the cells with broad substrate specificity (10). In 2002, Tseng et al. showed a correlation between early and advanced clinical stages and MDR1 expression in head and neck cancer (11). Recently, the correlation between MDR1 expression and poor response to MDR1-dependent chemotherapeutic drugs has been shown (12). For all these reasons, there is a need for novel therapeutic strategies that may improve the clinical outcome in head and neck cancer patients.

Received 11/15/06; revised 4/11/07; accepted 4/27/07.

Grant support: Austrian National Bank Project 11681; Austrian Cancer Society/Tyrol. Work in the laboratory of Prof. Lukas A. Huber is supported by the Austrian Proteomics Platform within the Austrian Genome Program, Vienna, Austria, and the Special Research Program ''Cell Proliferation and Cell Death in Tumors'' (SFB021, Austrian Science Fund).

The costs of publication of this article were defrayed in part by the payment of page charges. This article must therefore be hereby marked *advertisement* in accordance with 18 U.S.C. Section 1734 solely to indicate this fact.

Note: S. Skvortsov and I. Skvortsova contributed equally to this work.

Requests for reprints: Sergej Skvortsov, Department of Internal Medicine, Innsbruck Medical University, Anichstrasse 35, A-6020 Innsbruck, Austria. Phone: 43-512-504-25611; Fax: 43-512-504-25612. E-mail: Sergej.Skvortsov@i-med.ac.at

doi:10.1158/1535-7163.MCT-06-0708

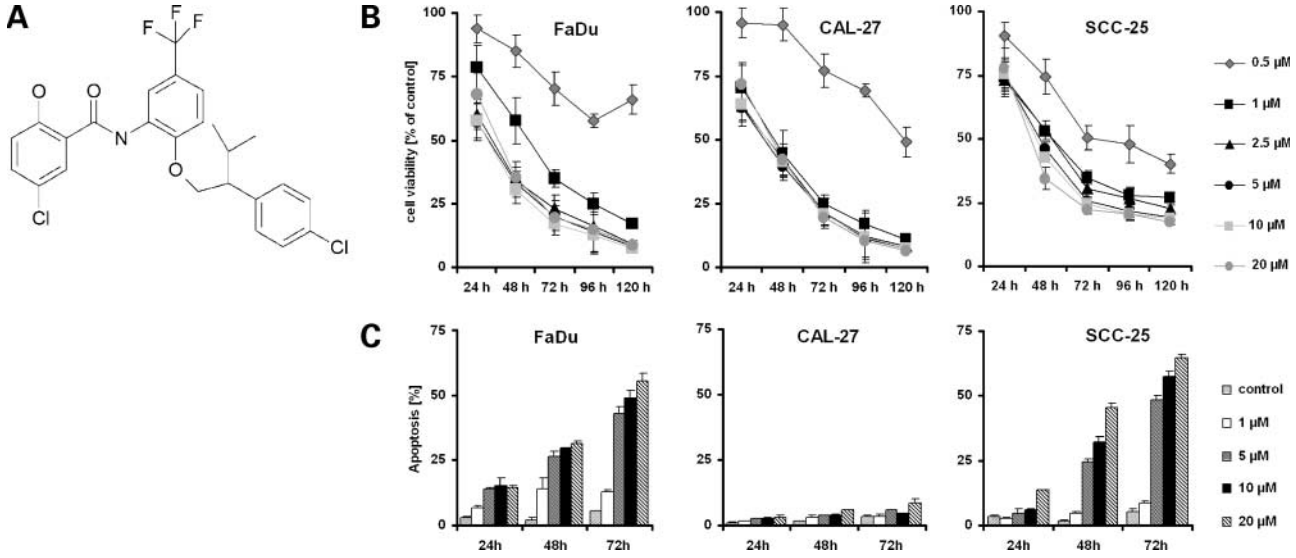

Figure 1. Structure of CTFB and effects on the cell growth and apoptosis of HNSCC. **A,** structure of CTFB. **B,** FaDu, CAL-27, and SCC-25 cells were treated with concentrations from 0.5 to 20 μmol/L for 0 – 120 h and subjected to photometry analysis using sulforhodamine B assay. The growth of cells was inhibited significantly in dose- and time-dependent manner in all cell lines. **C,** percentage of apoptotic cells was calculated by gating the sub-G_1 region on the DNA content histogram. *Columns,* mean obtained from three independent experiments; *bars,* SD.

5-Chloro-N-{2-[2-(4-chloro-phenyl)-3-methyl-butoxy]-5-trifluoromethyl-phenyl}-2-hydroxy-benzamide (CTFB) is a novel anticancer compound identified in a screen for inducers of apoptosis by Myriad Pharmaceuticals Inc. for the potential treatment of advanced solid tumors or hematologic malignancies (13). In experimental studies, CTFB showed significant killing activity in ovarian and prostate cancer cells as well as lymphoma cell lines. Additionally, CTFB showed significant inhibition of the growth of ovarian cancer cells in athymic nude mice xenografts.[7] When CTFB was tested to determine its susceptibility to MDR pumps, its anticancer activity in the MDR-expressed cell lines was similar to its activity in MDR-nonexpressed cell lines. Therefore, CTFB is not a substrate for MDR pumps (14).

To study the mechanisms of antitumor activity of CTFB, hypopharyngeal FaDu, tongue SCC-25, and CAL-27 squamous cell carcinoma cells were treated with CTFB. To identify the antiproliferative effects of CTFB and the mechanisms involved in the inhibition of cell growth, we identified differences in protein expression in head and neck squamous cancer cells (HNSCC) before and after treatment using fluorescent dye techniques such as two-dimensional difference gel electrophoresis (DIGE). Eight proteins that showed differential expression patterns in all cancer cell lines were identified using MALDI-TOF mass spectrometry. These proteins belong to different functional families that are involved in cytoskeleton formation and function and/or in cell cycle regulation. Furthermore, we show that antitumor activity of CTFB is associated with NF-κB down-regulation and proteasome activation. Our data show that proteome-based technologies represent a promising tool to investigate the complex interaction of the protein network in malignant cells after treatment with anticancer agents. *In vivo* experiments are in progress to further substantiate *in vitro* findings.

Materials and Methods

Cell Culture and Treatment with CTFB

The FaDu pharynx, SCC-25 and CAL-27 tongue squamous cancer cell lines were purchased from the American Type Culture Collection. FaDu cells were grown in EMEM with Earle's balanced salt solution (PAA Laboratories GmbH) supplemented with 2 mmol/L L-glutamine, 1.5 g/L sodium bicarbonate, 0.1 mmol/L nonessential amino acids, 50 units/mL penicillin, 50 μg/mL streptomycin, and 10% FCS (Sigma-Aldrich Handels GmbH). SCC-25 cells were maintained in a mixture of DMEM and Ham's F-12 medium (1:1, v/v; Invitrogen GmbH) containing 2.5 mmol/L L-glutamine, 15 mmol/L HEPES, 50 units/mL penicillin, 50 μg/mL streptomycin, and supplemented with 400 ng/mL hydrocortisone (Sigma-Aldrich Handels GmbH) and 10% FCS. CAL-27 cells were maintained in DMEM with 4 mmol/L L-glutamine adjusted to contain 1.5 g/L sodium bicarbonate and 4.5 g/L glucose (PAA Laboratories GmbH) and 10% FCS. Cultures were incubated in a 5% CO_2 humidified atmosphere.

5-Chloro-*N*-{2-[2-(4-chloro-phenyl)-3-methyl-butoxy]-5-trifluoromethyl-phenyl}-2-hydroxy-benzamide (CTFB; Fig. 1A) was provided by Myriad Pharmaceuticals Inc.. Because CTFB at a concentration of 1 μmol/L was sufficient for growth delay in viability assays and showed only weak apoptotic effects in FaDu cells, this dose was used for all further experiments.

[7] Pleiman et al., manuscript in preparation.

For statistical evaluation, mean values and SD were calculated using three independent experiments; significance was determined by paired Student's *t* test.

Viability Assay

Cultured cells with and without CTFB treatment were fixed with 50 μL per well ice-cold 50% trichloroacetic acid at 4°C overnight after 0, 24, 48, or 72 h. After washing five times with water and air-drying for ~20 min, cells were stained with 100 μL of 0.4% sulforhodamine B (Sigma-Aldrich Handels GmbH) in 1% acetic acid for 15 min. Subsequently, plates were washed five times with 1% acetic acid and air-dried, and the dye was resuspended in 100 μL of 10 mmol/L Tris buffer (pH, 10.5). Dye quantification was done with a microplate reader (SPECTRAFluor Plus, Tecan Austria GmbH) at 510 nm. Cell viability was calculated as follows: [experimental absorbance/untreated control absorbance] × 100 at each time point.

Protein Fractionation and Two-Dimensional DIGE

For sample preparation, cells were scraped and harvested by centrifuging at 4°C for 5 min at 100 × *g*. After washing by centrifugation with 10 mL of PBS containing protease inhibitors [1 mmol/L EDTA, 1 mmol/L phenylmethylsulfonyl fluoride (PMSF), 1 μg/mL leupeptin, 5 μg/mL aprotinin] cells were resuspended in 2 mL of homogenization buffer (250 mmol/L sucrose, 3 mmol/L imidazole [Sigma-Aldrich Handels GmbH] in double-distilled water) also containing the protease inhibitors and centrifuged for 10 min at 1,000 × *g* and 4°C. Cells were resuspended in homogenization buffer (thrice the volume of the cellular pellet) and homogenized using a 25-gauge needle attached to a 1-mL syringe. Homogenate was centrifuged at 1,700 × *g* for 10 min at 4°C, and the postnuclear supernatant was collected in a new tube. Total membrane proteins were obtained by ultracentrifugation of the postnuclear supernatant at 100,000 × *g* for 1 h at 4°C. Cytosolic fraction was collected in a new tube. The membrane pellet was washed with homogenization buffer by centrifugation at 100,000 × *g* for 40 min at 4°C and resuspended in homogenization buffer. Proteins both of cytosolic and membrane fractions were precipitated using methanol/chloroform as previously described (15). Precipitated proteins were then resolubilized in lysis solution [7 mol/L urea, 2 mol/L thiourea, 40 mmol/L Tris base, 1% C7BZO (Sigma-Aldrich Handels GmbH)]. Protein concentrations were determined with a commercially available kit (Bio-Rad Laboratories). About 30 μg of protein in 20 μL of lysis solution were labeled with 180 pmol of CyDye DIGE Fluor minimal dyes (Amersham Biosciences; Cy3, Cy5 for sample or Cy2 for internal control) for 30 min, resuspended in 280 μL of rehydration buffer [7 mol/L urea, 2 mol/L thiourea, 1% C7BZO, 0.5% immobilized pH gradient (IPG) buffer, DTT 60 mmol/L for cytosolic fraction, and 7 mol/L urea, 2 mol/L thiourea, 1% ASB-14 (Sigma-Aldrich Handels GmbH) and 0.5% IPG buffer, DTT 60 mmol/L for membrane fraction] and loaded on immobilized 18-cm pH 3–10 nonlinear (NL) gradient strips. For the first dimension, active rehydration (50 V) was carried out at 20°C for 12 h. Isoelectric focusing was done at 250 V for 30 min, 500 V for 1 h, 2000 V for 1 h, and finally at 8,000 V until 35,000 V/h were reached in total. For the second dimension, samples were separated on 12.5% polyacrylamide gels with the Ettan Dalttwelve System following the standard procedure recommended by the manufacturer (Amersham Biosciences). After electrophoresis, gels were scanned using a Typhoon 94100 Imager at 100 dpi resolution (Amersham Biosciences). Statistical analysis of changed proteins between samples was done using DeCyder difference in-gel analysis (DIA) and DeCyder biological variation analysis (BVA) software (Amersham Biosciences), setting the Student's *t* test to <0.05.

In-Gel Digestion and MALDI-TOF/TOF Protein Identification

Protein spots were excised from gels with the Ettan Spot Picker (Amersham Biosciences) and in-gel digested with trypsin (Promega) as described by Hellman (16). The in-gel digests were concentrated and desalted using microZipTipC18 (Millipore) by elution of peptides with the acetonitrile solution containing the α-cyano-4-hydroxycinnamic acid as a matrix directly onto the target. Mass spectra were acquired using a MALDI-TOF/TOF Ultraflex instrument (Bruker Daltonics). Peptide mass fingerprintings and MS/MS spectra of selected precursor ions were interpreted using MASCOT[8] against the National Center for Biotechnology Information nonredundant protein database.

Cell Cycle Analysis and Detection of Apoptosis

Exponentially growing cells were treated with CTFB for 24, 48, and 72 h in 10% FCS supplemented medium. About 5×10^5 cells per tube were pelleted at 200 × *g*, washed twice with PBS, stained in 500 μL of DNA staining solution (50 mg/mL propidium iodide, 0.1% Triton X-100, 0.1% sodium citrate), incubated in the dark for 30 min and kept at 4°C until fluorescence-activated cell sorting analysis. The propidium iodide fluorescence of individual nuclei was determined using a FACSCalibur with an excitation wavelength of 488 nm and an emission wavelength at 670 nm. Results were represented as DNA histograms for further analysis using CellQuest software (Becton Dickinson). Distribution of cells in the G_0-G_1, S, G_2-M phases of the cell cycle was determined using ModFit LT 3.0 (Verity Software House, Inc.).

Percentage of apoptotic cells was calculated by gating the sub-G_1 region on the DNA content histogram. Cell debris and small particles were excluded from the analysis.

Nuclear/Cytoplasmic Fractionation and Western Blot Analysis

For nuclear/cytoplasmic fractionations, 4×10^7 cells were lysed in 500 μL of cytoplasmic extract buffer [CEB; 10 mmol/L HEPES, 60 mmol/L KCl, 1 mmol/L EDTA, 1 mmol/L DTT, 1 mmol/L PMSF, 1 μg/mL leupeptin, 5 μg/mL aprotinin, 0.075% NP40 (Sigma-Aldrich Handels

[8] http://www.matrixscience.com/

GmbH); pH, 7.6] and incubated on ice for 3 min. After centrifugation at 200 × *g*, the cytoplasmic fractions were removed from the pellets to clean tubes and the nuclei washed with 1 mL of CEB without detergent. To the nuclear pellets, 500 μL of nuclear extract buffer [20 mmol/L Tris-HCl, 420 mmol/L NaCl, 1.5 mmol/L $MgCl_2$, 0.2 mmol/L EDTA, 1 mmol/L PMSF, 1 μg/mL leupeptin, 5 μg/mL aprotinin, 25% v/v glycerol (pH, 8.0)] was added and incubated on ice for 20 min. After centrifugation at 10,000 × *g* for 10 min at 4°C, supernatants were collected into clean tubes. Protein precipitation was done using methanol/chloroform as previously described (15). The pellet was then dissolved in the loading buffer. Protein concentrations were determined as described above. Western blots were done as published previously (17) using the following antibodies: rabbit anti–inhibitory κB-α (IκB-α), rabbit anti–NF-κB p105/p50, rabbit anti–NF-κB p65, mouse anti-cyclin D1 (Cell Signaling Technology, Inc.), mouse anti-p27/Kip1, mouse anti-p21/WAF1, and mouse anti-p53 (Lab Vision Corporation). Anti–α-tubulin (Oncogene Research) antibody was used as loading control for cytoplasmic and anti-histone H3 (FL-136; Santa Cruz Biotechnology, Inc.) for nuclear fractions. The bands were measured with a computerized digital imaging system using GelScan 5.1 software (Serva Electrophoresis). The integrated density value (IDV) was obtained as a ratio of protein band density to α-tubulin or histone H3 band density after background correction.

Fluorescence Microscopy

Treated and control cells were fixed for 15 min with 4% paraformaldehyde in PBS. Cells were washed with PBS and permeabilized for 15 min with 0.1% saponin in PBS containing 1% bovine serum albumin and 0.1% sodium azide. Cells were incubated at room temperature for 1 h with rabbit anti–phospho-NF-κB p65 (Ser^{536}) monoclonal antibody (Alexa Fluor 488 conjugate; Cell Signaling Technology, Inc.), washed twice, and coverslipped using a fluorescent mounting medium (DAKOCytomation GmbH). Slides were analyzed by confocal fluorescence microscopy (LSM 510 META, Carl Zeiss GmbH) using Zeiss LSM Software, version 3.2.

20S Proteasome Activity

To evaluate 20S proteasome activity, exponentially growing cells were treated with CTFB for 24, 48, and 72 h. Cells were pelleted at 200 × *g*, lysed for 15 min at 4°C in radioimmunoprecipitation assay buffer [50 mmol/L Tris-HCl (pH, 7.5), 150 mmol/L NaCl, 1 mmol/L EDTA, 1 mmol/L PMSF, 1 μg/mL leupeptin, 5 μg/mL aprotinin,

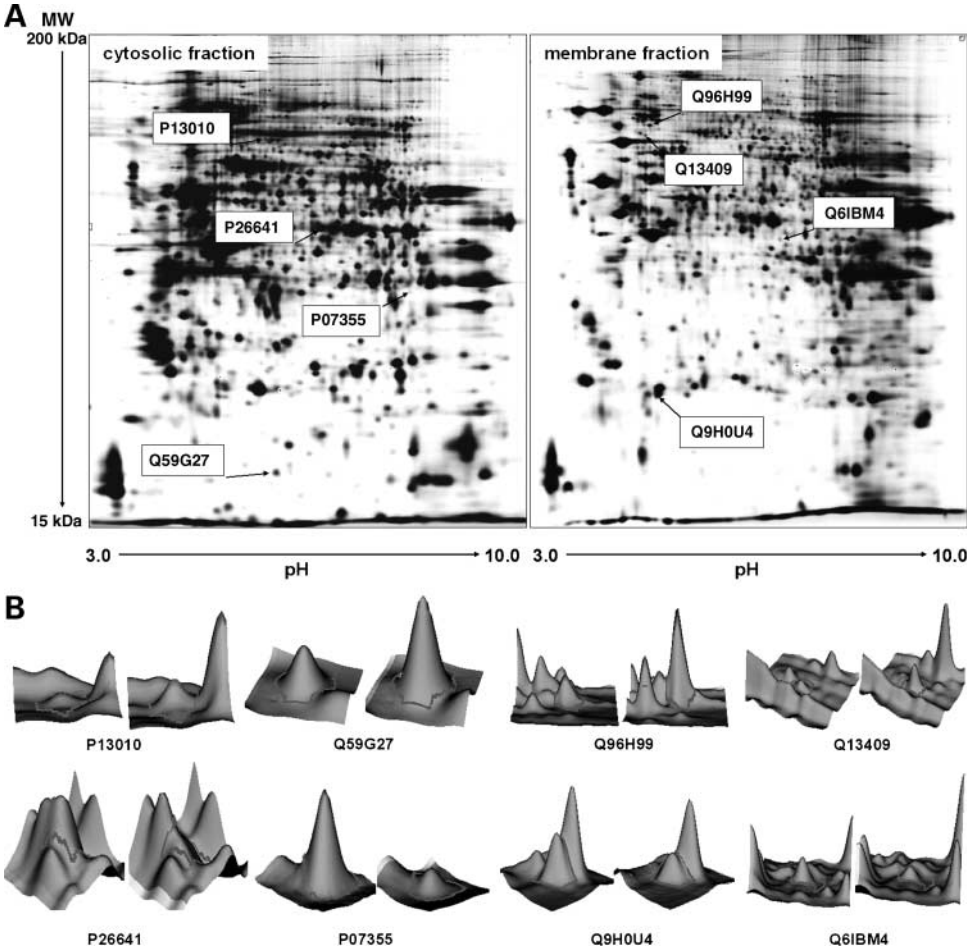

Figure 2. Protein images identified by two-dimensional DIGE. **A,** protein extracts from cytosolic and membrane fractions were labeled with either Cy3 (control) or Cy5 (CTFB treated for 24 h) and subjected to isoelectric focusing with a Cy2-labeled pooled standard using immobilized 18-cm, pH 3–10, NL gradient strips. For the second dimension, samples were separated on 12.5% polyacrylamide gels. *Arrows,* CTFB-regulated proteins with accession number (SWISS-Prot database). **B,** differentially expressed spots were evaluated from three independent experiments using DIA and BVA software setting Student's *t* test to <0.05. Corresponding identifications of proteins presented in Table 1.

Table 1. Function and expression of identified proteins

Target protein	Accession no.	MW (kDa)	Function	Regulation coefficient (after CTFB treatment)
Cytosolic fraction				
ATP-dependent DNA helicase II	P13010	83.2	Catalyzes the unwinding of parental DNA strands during replication, repair, recombination, and in some cases, transcription with intrinsic DNA-dependent ATPase activity	2.1
Stathmin 1 variant	Q50G27	17.3	Microtubule-destabilizing protein that promotes microtubule depolymerization	1.7
Eukaryotic translation elongation factor 1γ	P26641	50.1	Subunit of EF1, one of the G proteins that mediate the transport of aminoacyl tRNA to 80S ribosomes during translation	−1.8
Annexin A2	P07355	38.8	Calcium-regulated, F-actin– and phospholipid-binding protein; overexpression of annexin A2 plays a role in proliferation and metastasis development	−4.1
Membrane fraction				
Cortactin, isoform b	Q96H99	57.6	F-actin–binding protein; the function of the isoform b is not well understood	2.6
Cyoplasmic dynein intermediate chain	Q13409	68.7	Responsible for transporting of membranous vesicles and different cargoes to the minus end of microtubules, including endosomes, lysosomes; implicated in the positioning of the Golgi apparatus, centrosome localization, and microtubule transport	1.8
RAB1B, member RAS oncogene family	Q9H0U4	22.3	Serves as molecular switch to control the protein transport from the endoplasmic reticulum to Golgi complex and between Golgi compartment	−1.6
Heterogeneous nuclear ribonucleoprotein H	Q6IBM4	49.3	Acts as a major gene regulatory protein that binds heterogeneous nRNA and plays a fundamental role in controlling gene expression	−2.1

1% NP40, 0.5% deoxycholic acid sodium salt, 0.1% SDS] and sonified. After centrifugation at 10,000 × *g* for 10 min at 4°C, supernatants were collected and protein concentrations were determined as described above. Proteasome activity assays were done according to the assay instructions (CHEMICON Europe, Ltd.). Briefly, measurements of proteasome activities were done using the labeled substrate Suc-LLVY-AMC. Substrate Suc-LLVY-AMC was dissolved at 10 mmol/L in DMSO and then diluted 1:20 in assay buffer. Total cell lysates (20 μg) were diluted to 100 μL in assay buffer. Substrate Suc-LLVY-AMC were added to samples and incubated at 37°C for 1 h. Fluorescence intensities were measured with a microplate reader SpectraFluor Plus (Tecan Austria GmbH) using 380 nm excitation and 460-nm emission filters. Background readings from buffers were subtracted from the readings of each sample.

Inhibition of Proteasome Activity and Cell Proliferation Assay

Cultured cells (5×10^3 cells per well) were treated with CTFB at a concentration of 1 μmol/L or in combination with lactacystin at concentrations of 1, 5, or 10 μmol/L for 4 and 8 h at a total volume of 200 μL in 96-well flat-bottom plates. The proliferation was measured using bromodeoxyuridine (BrdUrd) incorporation assay [Cell Proliferation ELISA, BrdUrd (colorimetric); Roche Diagnostics GmbH]. The BrdUrd ELISA was done according to the manufacturer's instructions. Briefly, the cells were labeled with 20 μL of BrdUrd labeling solution for the last 2 h. After cultivation, cells were fixed with 200 μL of FixDenat solution for 30 min. After removing FixDenat, 100 μL of anti–BrdUrd-POD solution was added to each well. Following incubation for 90 min, 100 μL of substrate solution was added to each well. Absorbance of the samples was measured at 370 nm, a test wavelength, and at 492 nm, a reference wavelength, in a PowerWave XS microplate spectrophotometer (BioTek Instruments Inc.). The blank well corresponded to 100 μL of culture medium with BrdUrd and anti–BrdUrd-POD.

Results

Effects of CTFB on Cell Growth and Apoptosis

To determine the growth-inhibitory activity of CTFB, FaDu, SCC-25, and CAL-27, cells were treated with concentrations from 0.5 to 20 μmol/L and cell viability was assessed from 24 to 120 h of incubation. CTFB treatment was shown to inhibit cell growth in a time- and

dose-dependent manner in all cell lines (Fig. 1B). However, in FaDu and CAL-27 cell lines, CTFB at a concentration of 1 μmol/L was found to be the most potent with 17.16 ± 2.08% and 10.92 ± 1.22% of cells surviving at 120 h, respectively. Treatment of SCC-25 cells with 1 μmol/L CTFB revealed cell viability of 27.03 ± 1.86% at 120 h. Further increases in CTFB concentration to up to 20 μmol/L did not result in significant differences in growth inhibition in all cell line studies. To examine the effects of CTFB on apoptosis, the cells were treated at concentrations from 1 to 20 μmol/L for 24, 48, and 72 h (Fig. 1C). It is interesting to note that CTFB caused only an antiproliferative effect in the more sensitive CAL-27 cells with ~25% cell viability at 72 h without apoptosis development. FaDu and SCC-25 cells show dose- and time-dependent DNA degradation and apoptosis up to 55% and 65% at 72 h, respectively.

CTFB Changes Expression of Proteins Involved in Cytoskeleton and Cell Cycle Regulation

To identify potential mechanisms involved in CTFB-induced growth inhibition, cells were treated for 24 h, and the protein profiles of cytosolic and membrane fractions were examined by two-dimensional DIGE. Among the ~5,000 protein spots detected per cell line, up to 85 were up-regulated, and 82 were down-regulated proteins in cytosolic end membrane fractions. Proteins were selected for mass spectrometry analysis when the expression of individual proteins statistically differed by a ratio of more than 1.5 in all cell lines. The identity of four cytosolic proteins and four membrane proteins were determined. The identified proteins as well as their physical parameters and biological functions are summarized in Fig. 2A and B and Table 1. They belong to different structural or functional families and are involved in the control of cell cycle and cytoskeleton formation and function.

G_0-G_1 Arrest Is Associated with Up-regulation of p21/WAF1 and p27/Kip1 and Down-regulation of Cyclin D1

The distribution of cells in different phases of the cell cycle is shown in Fig. 3A. A more pronounced accumulation of cells in the G_0-G_1 phase was observed in the CAL-27 cells (74.88 ± 0.86% at 24 h; 80.08 ± 1.71% at 48 h; 79.33 ± 2.02% at 72 h) and FaDu cells (53.11 ± 1.47% at 24 h; 56.71 ± 0.46% at 48 h; 58.72 ± 4.02% at 72 h). Accumulation of cells in G_0-G_1 phase was accompanied by a decreased number of cells in S and G_2-M phases. Although SCC-25

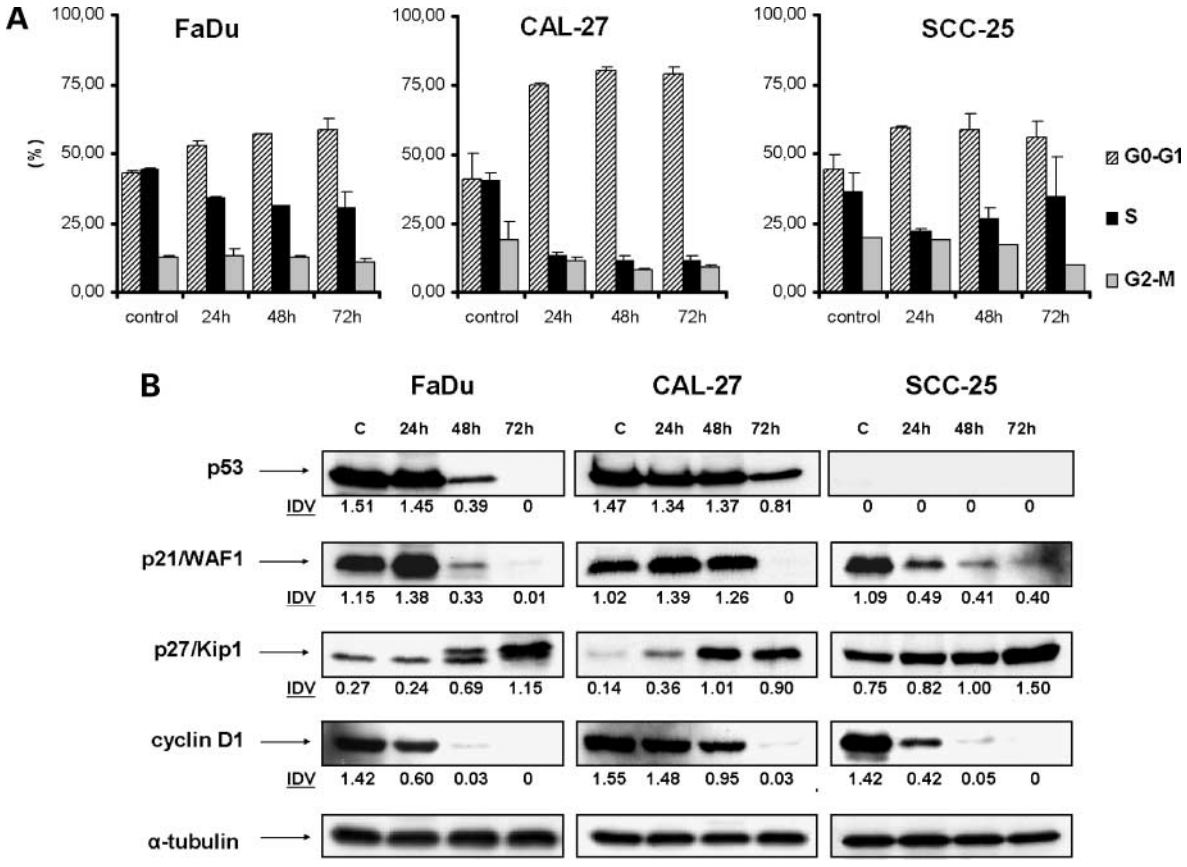

Figure 3. CTFB causes cell cycle perturbations in HNSCC cell lines. **A,** cell cycle regulation by CTFB treatment in HNSCC. FaDu, CAL-27, and SCC-25 cells were treated with 1 μmol/L CTFB, and cell cycle distribution was assessed during 72 h using flow cytometry as described in Materials and Methods. *Columns,* mean of three independent experiments; *bars,* SD. **B,** cell cycle–related protein expression. The cells were treated with CTFB for 24, 48, and 72 h and subjected to immunoblot analysis. IDV was calculated as a ratio of protein band density to α-tubulin after background correction.

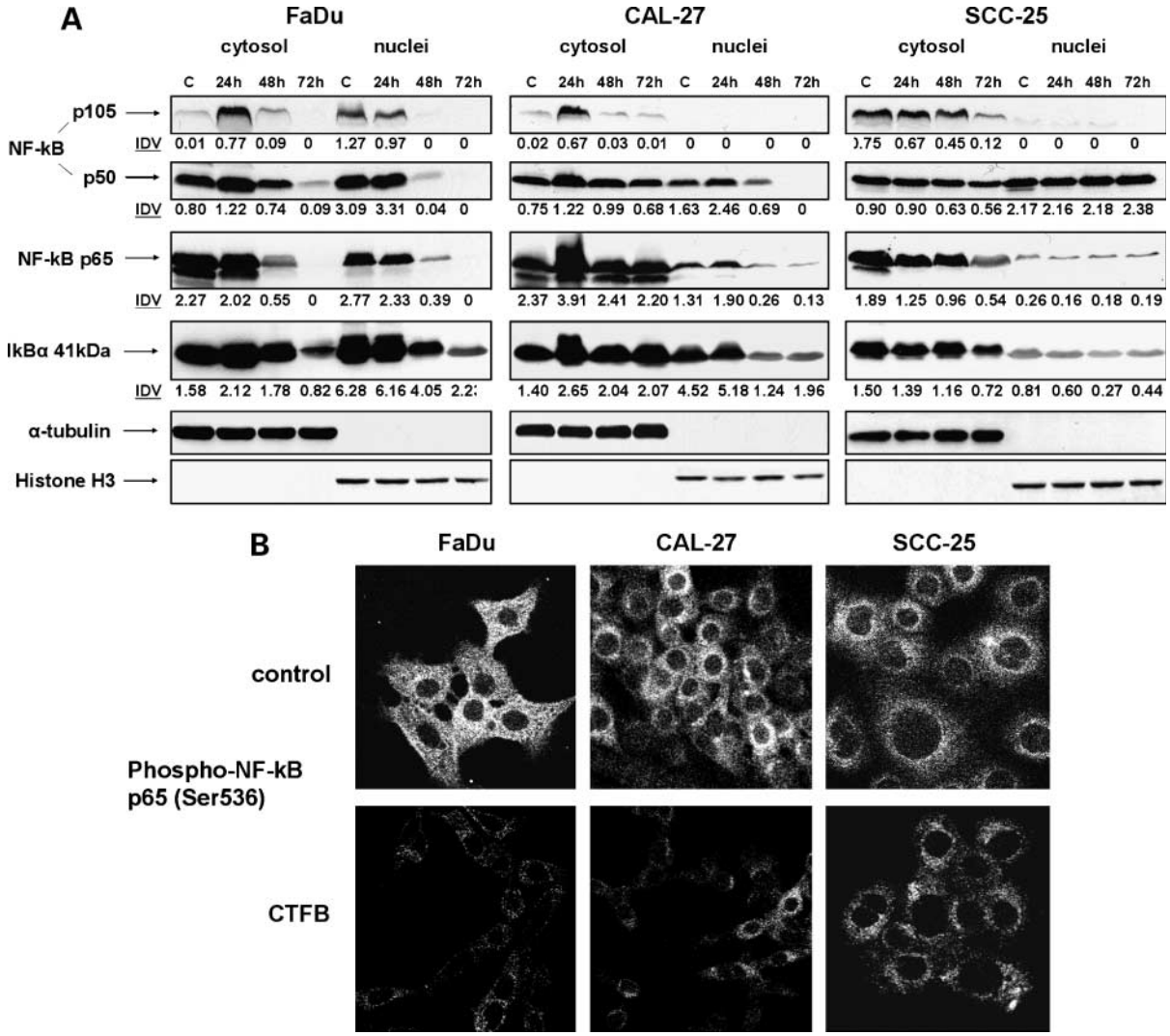

Figure 4. The effects of CTFB upon NF-κB expression. **A,** Western blot analysis of NF-κB and IκB-α cytoplasmic and nuclear fraction. The figure represents the level of expression of proteins by 0 h as control and after CTFB treatment over 72 h. IDV was calculated as a ratio of protein band density to α-tubulin or Histone H3 band density after background correction. **B,** cells were treated with 1 μmol/L CTFB for 24 h, fixed, and incubated with anti–phospho–NF-κB p65 (Ser^{536}) antibody. Samples were visualized by confocal fluorescence microscopy using a blue filter of 470–490 nm.

cells revealed G_0-G_1 cell cycle arrest at 24 h (59.09 ± 0.88%), cell accumulation at the G_0-G_1 phase slightly decreased to 58.43 ± 6.03% at 48 h and 55.86 ± 5.65% at 72 h with simultaneous increases in the number of cells in the S phase.

We next examined the expression of p53, p21/WAF1, p27/Kip1, and cyclin D1 proteins, which represent critical checkpoints in the G_1-S transition. As determined by immunoblotting, CTFB treatment decreased the expression of p53 in FaDu and CAL-27 cell lines. SCC-25 cells did not possess detectable levels of p53 (Fig. 3B). Expression of the cyclin-dependent kinase (Cdk) inhibitor p21/WAF1 was enhanced only at 24 h in FaDu and CAL-27 cells, whereas SCC-25 cells showed decreased levels of p21/WAF1 at 24–72 h. However, increases in the expression of p27/Kip1 were observed in a time-dependent manner in all cell lines. The expression of cyclin D1 significantly decreased following 72 h of CTFB treatment in all cell lines, which corresponded to the increases in p27/Kip1 expression.

CTFB Inhibits Tumor Cells Growth through the Down-regulation of NF-κB Expression and Enhancement of 20S Proteasome Activity

Due to the identification of proteins by two-dimensional DIGE that participate in the cell cycle regulation, we tested whether the transcription factor NF-κB is involved in CTFB-mediated cell growth inhibition. CTFB treatment inhibited both active cytosolic NF-κB p50 and NF-κB p65 forms in all cell lines (Fig. 4A). NF-κB p50 and NF-κB p65 were down-regulated in the nuclear fraction of CAL-27 and FaDu cells, whereas SCC-25 cells showed slightly increased

levels of NF-κB p50 at 24–72 h after treatment with CTFB. The expression of IκB-α strongly correlated with NF-κB expression in FaDu and CAL-27 cell lines. To define changes in the levels of phosphorylated NF-κB p65 [phospho–NF-κB p65 (Ser^{536})] upon CTFB treatment, cells were treated for 24 h, stained with rabbit anti–phospho–NF-κB p65 (Ser^{536}) monoclonal antibody and analyzed using immunofluorescent microscopy. For each cell line, identical microscopic parameters were used. In untreated cells, diffuse cytosol staining was observed (Fig. 4B). Phospho–NF-κB p65 (Ser^{536}) in FaDu and CAL-27 cells was markedly decreased after CTFB treatment. In contrast, SCC-25 cells did not show obvious changes in staining.

We then determined S20 proteasome activity in CTFB-treated cells. As shown in Fig. 5A, cell lines had different constitutive proteasome activity with 16,304 ± 843 relative fluorescent units (RFU) in CAL-27 cells, 13,247 ± 716 RFU in FaDu cells and 7,399 ± 591 RFU in SCC-25 cells. Lactacystin, a highly specific proteasome inhibitor, was used as a positive control and significantly inhibited proteasome activity in all tested cell lines. FaDu and CAL-27 cells showed the most prominent proteasome activation in response to CTFB treatment (18,114 ± 3,765 RFU at 24 h, 20,608 ± 2,194 RFU at 48 h, 29,928 ± 4,666 RFU at 72 h in FaDu cells and 23,479 ± 3,351 RFU at 24 h, 23,903 ± 2,074 RFU at 48 h, 33,682 ± 3,882 RFU at 72 h in CAL-27 cells). In contrast, proteasome activity in the SCC-25 cell line was only slightly enhanced by CTFB (10,321 ± 1,293 RFU at 72 h). To determine whether lactacystin treatment can rescue CTFB-induced growth delay, cells were treated with 1 μmol/L of CTFB as a control, or in combination with lactacystin at concentrations of 1, 5, or 10 μmol/L (Fig. 5B). CAL-27 and FaDu cells showed the most prominent CTFB-caused proteasome activity and showed newly synthesized DNA upon concomitant lactacystin treatment in a dose-dependent manner with maximum levels observed at 4 and 8 h, respectively. In contrast, in SCC-25 cells with low CTFB-induced proteasome activity, lactacystin treatment cannot abrogate the antiproliferative effect of CTFB. Our results show that the proteasome proteolytic activity correlates with NF-κB degradation and inhibition of cell growth. These findings suggest that NF-κB degradation and concomitant proteasome activation are critical factors in CTFB-induced cell growth inhibition.

Discussion

Despite the recent advances in chemoradiotherapy and antibody therapy (18), the prognosis for patients with

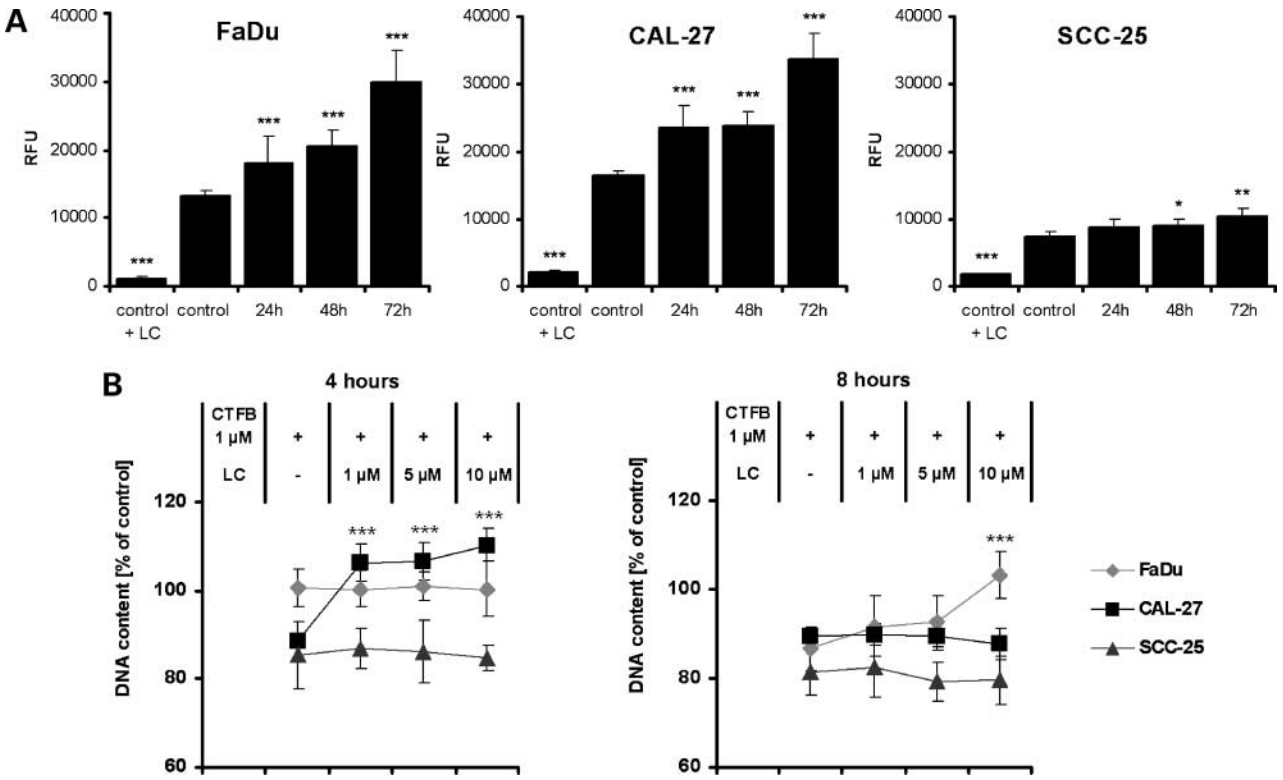

Figure 5. 20S proteasome activity and proliferation. **A,** the cells were treated with 1 μmol/L CTFB for 24, 48, and 72 h. Proteolytic activity of 20S proteasome was measured by the cleavage of the fluorogenic substrate Suc-LLVY-AMC. The proteasome activity was inhibited by lactacystin (*LC*) as positive control. **B,** the cells were treated with 1 μmol/L of CTFB or in combination with lactacystin. In CAL-27 and FaDu cell lines demonstrating most prominent proteasome activity, lactacystin can rescue newly synthesized DNA. *Columns,* mean from three independent experiments; *bars,* SD. *, $P < 0.05$; **, $P < 0.01$; ***, $P < 0.001$.

advanced squamous cell carcinoma of the oral cavity and pharynx is still poor (19). Therefore, the identification and targeting of molecular markers that predict response for new drug therapeutics are warranted (20). The purpose of this study was to investigate the antitumor effects of CTFB and to define the potential mechanism(s) of action involved in CTFB activity in head and neck cancer cells.

The head and neck cancer cell lines FaDu, SCC-25, and cisplatin-resistant CAL-27 (21) were used as representative of pharyngeal and tongue squamous cell carcinomas. The cisplatin-resistant cell line CAL-27 revealed the most significant cell growth delay in response to CTFB treatment. Analysis of the proteome profile revealed eight proteins with significant difference in expression level before and after CTFB treatment in all three cell lines.

The first protein was DNA helicase II, which is involved in transient unwinding of the double-stranded DNA into a single-stranded form for processes such as DNA replication, DNA repair, DNA recombination, and transcription (22). Our observations that DNA helicase II was up-regulated after CTFB treatment suggests that DNA helicase II may be involved in DNA repair that usually accompanies cytotoxic stress.

Another up-regulated protein, stathmin, regulates rapid microtubule remodeling of the cytoskeleton, tubulin sequestration, and catastrophe-promoting activities, which is also important for proper mitosis and other cellular processes (23). Several studies have shown that overexpression or inhibition of stathmin results in mitotic arrest. It was also shown that overexpression of stathmin results in growth suppression and accumulation of cells in the G_2-M phases of the cell cycle (24). Increases in stathmin expression after CTFB treatment may be responsible for delays in cell growth and cell cycle arrest in G_0-G_1 phase.

Eukaryotic translation elongation factor 1γ (EF-1γ) plays an important role in translation by mediating the transport of aminoacyl tRNA to 80S ribosomes and is overexpressed in a high proportion in tumors at the mRNA and the protein level (25). It was shown that EF-1γ interacts with membrane and cytoskeleton structures in the cell and is involved in protein synthesis during G_2-M transition (26). The down-regulation of EF-1γ in HNSCC after CTFB treatment suggests that this protein is involved in the cell cycle control, which is characterized by cell accumulation at the G_0-G_1 phase.

Annexin A2 is also known as a calcium-regulated filamentous actin (F-actin)– and phospholipid-binding protein with a non-membranous cytosolic cellular distribution. Additionally, annexin A2 is a target of protein kinase C (27). Recently, it has been reported that annexin A2 is highly expressed in different kinds of cancers and correlates with the invasive potential and metastatic activity in head and neck cancer (28). A correlation between annexin A2 and cell proliferation is also shown in other systems, and down-regulation of annexin A2 by CTFB treatment is related to the impairment in cell proliferation.

Cortactin is another F-actin–binding protein and a substrate of Src tyrosine kinase, which is involved in actin arrangement in response to tyrosine kinase signaling and promotes actin polymerization by activating the Arp2/3 complex (29). Overexpression of cortactin promotes tumor cell dissemination and correlates with poor prognosis in HNSCC (30). It has been previously shown in MDA-MB-231 breast cancer cells infected with viral constructs that overexpression of cortactin has no effect on cell proliferation (31). In contrast, in our experiments, increased expression of the b isoform of cortactin following treatment with CTFB may have isoform-specific effects on the cell cycle.

Cytoplasmic dyneins are the major class of cytoskeleton-based motors that are responsible for the transport of a number of different cargoes to the minus-end of microtubules and implicated in the positioning of the Golgi apparatus and transport of microtubules (32). It was shown that changes in expression of the cytoplasmic dynein intermediate chain mRNA is associated with cellular senescence, but not with cell growth arrest induced by gamma-irradiation (33). In our experiments CTFB-induced cell growth arrest in HNSCC was accompanied by increases in expression of the cytoplasmic dynein intermediate chain protein.

Rab proteins form the largest group of the small G protein superfamily and belong to RAS oncogene family. Rab proteins are important regulators of vesicular transport, which is central to the interaction of cells with their environment and critical between the intracellular organelles (34). Moreover, some of them are essential for cell viability and local organization of the actin cytoskeleton. Here, we have shown that CTFB-induced cell growth delay was observed concomitantly with decreased expression of RAB1B protein.

The full range of function of the heterogeneous nuclear ribonucleoprotein (hnRNP) family is still unknown, and hnRNP-H is one of the lesser known members. Although normal epithelium cells express undetectable level of the protein, it was found that tumors derived from these tissues express this protein (35). The present study shows that hnRNP-H is down-regulated following treatment of cells with CTFB, which may modulate proteins involved in cell growth delay.

Because all these eight proteins are involved in cytoskeleton formation and function and cell cycle regulation, we further investigated the action of CTFB on other cell cycle–regulated proteins. Cell cycle progression is mediated by various Cdks and cyclins that enable progression from G_1 to S phase (36). Their activity is regulated by Cdk inhibitors such p21/WAF1 and p27/Kip1 (37). In the present study, the simultaneous up-regulation of p21/WAF1 and p27/Kip1 expression in FaDu and CAL-27 cells and the inhibition of cyclin D1 expression after CTFB treatment show that the growth inhibitory effect is mediated via G_0-G_1 phase cell cycle arrest. In contrast, SCC-25 cells revealed only increases in p27/Kip1 protein levels, which seemed to be independent of p53 expression because SCC-25 cells possess inactivating mutations in p53 (38).

Inhibition of cyclin D1 expression in SCC-25 cells did not inhibit transition to S phase cell cycle, suggesting that other signaling pathway such as the NF-κB may be involved in cell cycle progression in this cell line.

NF-κB represents a group of structurally related and evolutionary conserved proteins with transcriptional activity involved in the regulation of important processes such as inflammation, innate immunity, cell proliferation, and apoptosis (39). Constitutive NF-κB activity detected in tumor cells protects them from the induction of apoptosis and is an important molecular switch for the development of HNSCC (40). The nuclear translocation and DNA binding activities of NF-κB are inhibited through association with a member of the IκB family. Phosphorylation of IκB via the ubiquitin-proteasome pathway and nuclear translocation of active homo- or heterodimers triggers the resynthesis of IκB-α, giving rise to an autoregulatory loop that terminates the activation processes (41). It was reported that IκB-α binds the NF-κB p50/p65 heterodimer with 60-fold higher affinity than NF-κB p50/p50 homodimer (42). Moreover, IκB-α can bind to NF-κB p50 but does not block DNA binding (43). In our experiments, we show that the expression of NF-κB p50 and NF-κB p65, which have the potential to form heterodimers in the more CTFB-sensitive FaDu and CAL-27 cell lines, was significantly decreased both in cytosolic and nuclear fractions. Increased expression of NF-κB p50 in the nuclei of CTFB treated SCC-25 cells may result in only p50/p50 homodimer formation that is accompanied by a reduced response to CTFB treatment. Recently, it was shown that the nuclear translocation of NF-κB p65 phosphorylated at Ser^{536} was not associated with either IκB-α or NF-κB p50 regulation (44). In our study, CTFB caused a more pronounced decrease in NF-κB p65 phosphorylated at Ser^{536} in both cytosolic and nuclear fractions of FaDu and CAL-27 cells, which is in contrast to less CTFB-sensitive SCC-25 cell line.

Proteolytic degradation is critical to the maintenance of appropriate levels of regulatory proteins, and the 26S proteasome is capable of degrading most ubiquitinated proteins in the cells (45). The most commonly accepted model for NF-κB function suggests that the transcription factor is inhibited through association with a member of the IκB family. IκBs are phosphorylated under certain conditions and become targets for ubiquitination and subsequent proteasome-mediated degradation. This event enables the nuclear translocation of homo- or heterodimers of NF-κB and DNA binding activity (46). The essential role of proteasome in degradation of IκB-α and activation of NF-κB was suggested using proteasome inhibitor bortezomib in HNSCC (47). In contrast, there are also many reports showing alternative NF-κB pathways. To this point, it has been shown that the proteasome inhibitors induce IκB degradation and NF-κB transcriptional activation (48), and that NF-κB activation has been required for cisplatin-induced apoptosis in HNSCC (49). Similarly, it was shown that serum factor-mediated apoptosis was accompanied by increases in the expression of 26S proteasome subunits and subsequent NF-κB activation in histiocytoma cells (50). Based on our results demonstrating that cell growth delay correlated with CTFB-induced proteasome activation, we can assume that proteasome activation may be involved in NF-κB protein degradation via unknown mechanisms.

In conclusion, although the mechanisms of CTFB activity are not completely understood, the compound activates mechanisms leading to the collapse in cell division. CTFB promotes its antitumor effects through multiple pathways, such as cytoskeleton disruption, activation of Cdk inhibitors, proteasome activation, and down-regulation of NF-κB. All these properties make CTFB potentially attractive to be used as a component of the treatment of head and neck cancer.

References

1. Lefebvre JL. Current clinical outcomes demand new treatment options for SCCHN. Ann Oncol 2005;16 Suppl 6:vi7 – 12.
2. Raguse JD, Gath HJ, Oettle H, Bier J. Oxaliplatin, folinic acid and 5-fluorouracil (OFF) in patients with recurrent advanced head and neck cancer: a phase II feasibility study. Oral Oncol 2006;42:614 – 8.
3. Bourhis J, Rivera F, Mesia R, et al. Phase I/II study of cetuximab in combination with cisplatin or carboplatin and fluorouracil in patients with recurrent or metastatic squamous cell carcinoma of the head and neck. J Clin Oncol 2006;24:2866 – 72.
4. Bonner JA, Harari PM, Giralt J, et al. Radiotherapy plus cetuximab for squamous-cell carcinoma of the head and neck. N Engl J Med 2006;354: 567 – 78.
5. Browman GP, Hodson DI, Mackenzie RJ, Bestic N, Zuraw L. Choosing a concomitant chemotherapy and radiotherapy regimen for squamous cell head and neck cancer: a systematic review of the published literature with subgroup analysis. Head Neck 2001;23:579 – 89.
6. Bourhis J, Armand C, Pignon JP. Update of MACH-NC (Meta-analysis of Chemotherapy in Head and Neck Cancer) database focused on concomitant chemoradiotherapy [abstract 5505]. J Clin Oncol, American Society of Clinical Oncology Annual Meeting Proceedings (Post-Meeting Edition) 2004;22(Suppl S):489S.
7. Mandal M, Younes M, Swan EA, et al. The Akt inhibitor KP372-1 inhibits proliferation and induces apoptosis and anoikis in squamous cell carcinoma of the head and neck. Oral Oncol 2006;42:430 – 9.
8. Sharma H, Sen S, Muzio LL, Mariggio A, Singh N. Antisense-mediated down-regulation of anti-apoptotic proteins induces apoptosis and sensitizes head and neck squamous cell carcinoma cells to chemotherapy. Cancer Biol Ther 2005;4:720 – 7.
9. Aggarwal S, Takada Y, Singh S, Myers JN, Aggarwal BB. Inhibition of growth and survival of human head and neck squamous cell carcinoma cells by curcumin via modulation of nuclear factor-κB signaling. Int J Cancer 2004;111:679 – 92.
10. Tsuruo T, Naito M, Tomida A, et al. Molecular targeting therapy of cancer: drug resistance, apoptosis and survival signal. Cancer Sci 2003; 94:15 – 21.
11. Tseng CP, Cheng AJ, Chang JT, et al. Quantitative analysis of multidrug-resistance mdr1 gene expression in head and neck cancer by real-time RT-PCR. Jpn J Cancer Res 2002;93:1230 – 6.
12. Schmidt M, Schler G, Gruensfelder P, Hoppe F. Differential gene expression in a paclitaxel-resistant clone of a head and neck cancer cell line. Eur Arch Otorhinolaryngol 2006;263:127 – 34.
13. Bajji A, Arranz E, Srinivasan J, Delmar E, inventors; Myriad Genetics Inc., assignee. Compounds, compositions, and methods employing same. International publication number WO/2004/006858; 2004.
14. Roth B, Baichwal V, Pleiman, CM, inventors; Myriad Genetics Inc., assignee. Methoods of treating cancer. International publication number WO/2006/071954; 2004.
15. Wessel D, Flugge UI. A method for the quantitative recovery of protein in dilute solution in the presence of detergents and lipids. Anal Biochem 1984;138:141 – 3.

16. Hellman U. Sample preparation by SDS/PAGE and in-gel digestion. EXS 2000;88:43 – 54.

17. Skvortsov S, Skvortsova I, Sarg B, et al. Irreversible pan-ErbB tyrosine kinase inhibitor CI-1033 induces caspase-independent apoptosis in colorectal cancer DiFi cell line. Apoptosis 2005;10: 1175 – 86.

18. Caponigro F, Milano A, Basile M, Ionna F, Iaffaioli RV. Recent advances in head and neck cancer therapy: the role of new cytotoxic and molecular-targeted agents. Curr Opin Oncol 2006;18:247 – 52.

19. Malone JP, Stephens JA, Grecula JC, et al. Disease control, survival, and functional outcome after multimodal treatment for advanced-stage tongue base cancer. Head Neck 2004;26:561 – 72.

20. Thomas GR, Nadiminti H, Regalado J. Molecular predictors of clinical outcome in patients with head and neck squamous cell carcinoma. Int J Exp Pathol 2005;86:347 – 63.

21. Gioanni J, Fischel JL, Lambert JC, et al. Two new human tumor cell lines derived from squamous cell carcinomas of the tongue: establishment, characterization and response to cytotoxic treatment. Eur J Cancer Clin Oncol 1988;24:1445 – 55.

22. Thommes P, Hubscher U. Eukaryotic DNA helicases: essential enzymes for DNA transactions. Chromosoma 1992;101:467 – 73.

23. Howell B, Larsson N, Gullberg M, Cassimeris L. Dissociation of the tubulin-sequestering and microtubule catastrophe-promoting activities of oncoprotein 18/stathmin. Mol Biol Cell 1999;10:105 – 18.

24. Rubin CI, Atweh GF. The role of stathmin in the regulation of the cell cycle. J Cell Biochem 2004;93:242 – 50.

25. Mathur S, Cleary KR, Inamdar N, et al. Overexpression of elongation factor-1γ protein in colorectal carcinoma. Cancer 1998;82:816 – 21.

26. Janssen GM, Moller W. Elongation factor 1 β γ from *Artemia*. Purification and properties of its subunits. Eur J Biochem 1988;171: 119 – 29.

27. Gerke V, Moss SE. Annexins: from structure to function. Physiol Rev 2002;82:331 – 71.

28. Wu W, Tang X, Hu W, et al. Identification and validation of metastasis-associated proteins in head and neck cancer cell lines by two-dimensional electrophoresis and mass spectrometry. Clin Exp Metastasis 2002;19:319 – 26.

29. Daly RJ. Cortactin signalling and dynamic actin networks. Biochem J 2004;382:13 – 25.

30. Rodrigo JP, Garcia LA, Ramos S, Lazo PS, Suarez C. EMS1 gene amplification correlates with poor prognosis in squamous cell carcinomas of the head and neck. Clin Cancer Res 2000;6:3177 – 82.

31. Li Y, Tondravi M, Liu J, et al. Cortactin potentiates bone metastasis of breast cancer cells. Cancer Res 2001;61:6906 – 11.

32. King SJ, Bonilla M, Rodgers ME, Schroer TA. Subunit organization in cytoplasmic dynein subcomplexes. Protein Sci 2002;11:1239 – 50.

33. Horikawa I, Parker ES, Solomon GG, Barrett JC. Up-regulation of the gene encoding a cytoplasmic dynein intermediate chain in senescent human cells. J Cell Biochem 2001;82:415 – 21.

34. Takai Y, Sasaki T, Matozaki T. Small GTP-binding proteins. Physiol Rev 2001;81:153 – 208.

35. Honore B, Baandrup U, Vorum H. Heterogeneous nuclear ribonucleoproteins F and H/H′ show differential expression in normal and selected cancer tissues. Exp Cell Res 2004;294:199 – 209.

36. Knudsen KE, Diehl JA, Haiman CA, Knudsen ES. Cyclin D1: polymorphism, aberrant splicing and cancer risk. Oncogene 2006;25: 1620 – 8.

37. Ekholm SV, Reed SI. Regulation of G(1) cyclin-dependent kinases in the mammalian cell cycle. Curr Opin Cell Biol 2000;12:676 – 84.

38. Ferguson BE, Oh DH. Proficient global nucleotide excision repair in human keratinocytes but not in fibroblasts deficient in p53. Cancer Res 2005;65:8723 – 9.

39. Ghosh S, Karin M. Missing pieces in the NF-κB puzzle. Cell 2002;109: S81 – 96.

40. Chang AA, Van Waes C. Nuclear factor-κB as a common target and activator of oncogenes in head and neck squamous cell carcinoma. Adv Otorhinolaryngol 2005;62:92 – 102.

41. Kucharczak J, Simmons MJ, Fan Y, Gelinas C. To be, or not to be: NF-κB is the answer-role of Rel/NF-κB in the regulation of apoptosis. Oncogene 2003;22:8961 – 82.

42. Malek S, Huxford T, Ghosh G. IκBα functions through direct contacts with the nuclear localization signals and the DNA binding sequences of NF-κB. J Biol Chem 1998;273:25427 – 35.

43. Bell S, Matthews JR, Jaffray E, Hay RT. I(κ)B(γ) inhibits DNA binding of NF-κB p50 homodimers by interacting with residues that contact DNA. Mol Cell Biol 1996;16:6477 – 85.

44. Sasaki CY, Barberi TJ, Ghosh P, Longo DL. Phosphorylation of RelA/p65 on serine 536 defines an IκBα-independent NF-κB pathway. J Biol Chem 2005;280:34538 – 47.

45. Krappmann D, Scheidereit C. A pervasive role of ubiquitin conjugation in activation and termination of IκB kinase pathways. EMBO Rep 2005;6: 321 – 26.

46. Chen Z, Hagler J, Palombella VJ, et al. Signal-induced site-specific phosphorylation targets IκBα to the ubiquitin-proteasome pathway. Genes Dev 1995;9:1586 – 97.

47. Lun M, Zhang PL, Pellitteri PK, et al. Nuclear factor-κB pathway as a therapeutic target in head and neck squamous cell carcinoma: pharmaceutical and molecular validation in human cell lines using Velcade and siRNA/NF-κB. Ann Clin Lab Sci 2005;35:251 – 8.

48. Nemeth ZH, Wong HR, Odoms K, et al. Proteasome inhibitors induce inhibitory κB (IκB) kinase activation, IκBα degradation, and nuclear factor κB activation in HT-29 cells. Mol Pharmacol 2004;65:342 – 9.

49. Kim SB, Kim JS, Lee JH, et al. NF-κB activation is required for cisplatin-induced apoptosis in head and neck squamous carcinoma cells. FEBS Lett 2006;580:311 – 8.

50. Singh S, Khar A. Activation of NFκB and Ub-proteasome pathway during apoptosis induced by a serum factor is mediated through the up-regulation of the 26S proteasome subunits. Apoptosis 2006;11:845 – 59.

Molecular Cancer Therapeutics

Antitumor activity of CTFB, a novel anticancer agent, is associated with the down-regulation of nuclear factor- κB expression and proteasome activation in head and neck squamous carcinoma cell lines

Sergej Skvortsov, Ira Skvortsova, Taras Stasyk, et al.

Mol Cancer Ther 2007;6:1898-1908.